DOI: 10.1534/genetics.104.035089

MuDR Transposase Increases the Frequency of Meiotic Crossovers in the Vicinity of a *Mu* Insertion in the Maize *a1* Gene

Marna D. Yandeau-Nelson,* Qing Zhou,*,[1] Hong Yao,*,[2] Xiaojie Xu,†,[3] Basil J. Nikolau*,†,‡ and Patrick S. Schnable*,†,§,,[4]**

*Interdepartmental Genetics Program, †Molecular, Cellular and Developmental Biology Program, ‡Department of Biochemistry, Biophysics and Molecular Biology, §Department of Agronomy and **Center for Plant Genomics, Iowa State University, Ames, Iowa 50011

Manuscript received August 17, 2004
Accepted for publication October 19, 2004

ABSTRACT

Although DNA breaks stimulate mitotic recombination in plants, their effects on meiotic recombination are not known. Recombination across a maize *a1* allele containing a nonautonomous *Mu* transposon was studied in the presence and absence of the *MuDR*-encoded transposase. Recombinant *A1′* alleles isolated from *a1-mum2/a1::rdt* heterozygotes arose via either crossovers (32 CO events) or noncrossovers (8 NCO events). In the presence of *MuDR*, the rate of COs increased fourfold. This increase is most likely a consequence of the repair of *MuDR*-induced DNA breaks at the *Mu1* insertion in *a1-mum2*. Hence, this study provides the first *in vivo* evidence that DNA breaks stimulate meiotic crossovers in plants. The distribution of recombination breakpoints is not affected by the presence of *MuDR* in that 19 of 24 breakpoints isolated from plants that carried *MuDR* mapped to a previously defined 377-bp recombination hotspot. This result is consistent with the hypothesis that the DNA breaks that initiate recombination at *a1* cluster at its 5′ end. Conversion tracts associated with eight NCO events ranged in size from <700 bp to >1600 bp. This study also establishes that *MuDR* functions during meiosis and that ratios of CO/NCO vary among genes and can be influenced by genetic background.

GENES are recombination hotspots in bacteria, fungi, plants, and animals (reviewed by Lichten and Goldman 1995; Schnable *et al.* 1998). For example, the ratio between genetic and physical distances within the maize *a1* gene is 6.25 cM/Mb (Civardi *et al.* 1994), as compared to the genome average of 2.4 cM/Mb, a figure that is based on a maize genetic map that consists of 5917 cM (Lee *et al.* 2002). Recombination breakpoints are not evenly distributed across some of these genic hotspots (Eggleston *et al.* 1995; Patterson *et al.* 1995; Xu *et al.* 1995). For example, a 377-bp sequence at the 5′ coding region of the *a1* locus is a recombination hotspot that exhibits a recombination rate of 16.1 cM/Mb (Xu *et al.* 1995).

Recombination events are of two types: reciprocal crossovers (COs) or nonreciprocal noncrossovers (NCOs), such as gene conversions. Detailed analyses of gene conversion events in Drosophila and fungi have established that: (1) conversion tract lengths are relatively short and continuous [*e.g.*, they average ~350 bp in Drosophila (Hilliker *et al.* 1994)] and (2) gene conversions exhibit a phenomenon termed polarity [*e.g.*, DNA sequences near one end of the *rosy* locus of Drosophila and the *ARG4* and *HIS4* loci of yeast (Schultes and Szostak 1990; Detloff *et al.* 1992) exhibit higher rates of gene conversion than do sequences at the other end of these loci]. In most cases, higher frequencies occur at the 5′ ends of these genes.

In most plants, gene conversion and double-crossover events cannot be distinguished. Even so, in the absence of strong negative interference, intragenic double crossovers are expected to occur only very rarely. Although putative gene conversions were reported in maize as early as 1986 (Dooner 1986), only a few conversion tracts have been molecularly characterized (Xu *et al.* 1995; Dooner and Martinez-Ferez 1997b; Mathern and Hake 1997; Li *et al.* 2001; Yao *et al.* 2002).

Several models have been proposed to explain the mechanism responsible for meiotic recombination (Holliday 1964; Resnick 1976; Szostak *et al.* 1983). The most widely accepted of these are based upon the double-strand break (DSB) repair model (Szostak *et al.* 1983; Sun *et al.* 1991) in which differential resolution of double-Holliday junction (DHJ) intermediates results in COs or NCOs. Evidence in support of this model has been obtained from the yeast *Saccharomyces cerevisiae* and other simple model organisms. The meiosis-induced

[1]*Present address:* BASF Plant Sciences, Research Triangle Park, NC 27709.

[2]*Present address:* Department of Biological Sciences, University of Missouri, Columbia, MO 65211.

[3]*Present address:* Department of Pathology, University of Wisconsin, Madison, WI 53706.

[4]*Corresponding author:* 2035B Roy J. Carver Co-Laboratory, Iowa State University, Ames, IA 50011. E-mail: schnable@iastate.edu

DSBs predicted by this model to initiate meiotic recombination have been observed at a number of loci (Sun *et al.* 1989, 1991; Game 1992; Zenvirth *et al.* 1992; de Massy and Nicolas 1993; Fan *et al.* 1995; Liu *et al.* 1995). Moreover, several studies have demonstrated the existence of recombination intermediates of the types postulated in the model, *i.e.*, joint molecules (Collins and Newlon 1994; Schwacha and Kleckner 1994; Schwacha and Kleckner 1995) and heteroduplex DNA (White *et al.* 1985; Lichten *et al.* 1990; Goyon and Lichten 1993; Nag and Petes 1993). More recently, Allers and Lichten (2001) proposed a modified DSB repair model. In this model, COs and NCOs are similarly initiated by DSBs but following resection and single end invasion (SEI) only some result in DHJs that can resolve as COs; the remainder are processed via the synthesis-dependent strand annealing pathway and resolve as NCOs. The identification of SEI intermediates in meiosis provides physical evidence for this modified model (Hunter and Kleckner 2001). This model is further supported by the identification of meiotic-related mutants that disrupt SEI formation and drastically reduce the production of COs but not NCOs (Borner *et al.* 2004).

It is thought that meiotic recombination in plants shares at least some mechanistic aspects with yeast (Xu *et al.* 1995; Puchta *et al.* 1996; Puchta and Hohn 1996). Due to technical barriers, less is known about the molecular nature of meiotic recombination in plants than in simple model organisms. Meiotic recombination hotspots in *S. cerevisiae* correspond to nearby DSB hotspots (reviewed in Lichten and Goldman 1995) that have been recently mapped throughout the genome (Gerton *et al.* 2000). Available techniques have thus far limited our ability to map DSBs in plants. Therefore, the possible association between DNA breaks and meiotic recombination hotspots in plants has not yet been established. Instead, meiotic recombination hot- and cold-spots are identified by physically mapping recombination breakpoints.

Although DSBs have not yet been mapped in plants, there is evidence that DNA breaks play a role in meiotic recombination. For example, processes that enhance the rate of DSB formation stimulate recombination in plants. This conclusion is based on three findings. First, agents that can physically (*e.g.*, X rays and UV irradiation) or chemically (*e.g.*, methylmethanesulfonate and mitomycin C) induce DSBs are able to stimulate intrachromosomal recombination (reviewed in Puchta and Hohn 1996). Second, the expression of the site-specific endonuclease I-*Sce*I in tobacco protoplasts (Puchta *et al.* 1993, 1996) and HO in somatic cells of Arabidopsis (Chiurazzi *et al.* 1996) increases the rates of mitotic recombination. Third, autonomous transposons have the ability to increase the rates of recombination-like losses of duplicated regions surrounding corresponding nonautonomous transposons in Arabidopsis and maize (Athma and Peterson 1991; Lowe *et al.* 1992; Stinard *et al.* 1993; Xiao *et al.* 2000; Xiao and Peterson 2000). Because these events either occurred in the absence of meiosis (Athma and Peterson 1991; Xiao *et al.* 2000; Xiao and Peterson 2000) or did not involve the exchange of flanking markers (Lowe *et al.* 1992) and therefore did not involve meiotic crossovers, they do not address the question as to whether DSBs stimulate meiotic recombination. Indeed, Dooner and Martinez-Ferez (1997a) have reported that meiotic recombination at the *bz1* locus in maize is not stimulated by the germinal excisions of the *Ac* transposon, which would be expected to introduce DSBs within *bz1*. The relationship between transposon excision and the stimulation of repair by recombination has not yet been elucidated in other transposon systems in maize.

The *a1* locus of maize is an excellent system for the study of meiotic recombination because: (1) intragenic recombination events can be easily identified by their visible nonparental phenotypes (*i.e.*, colored *vs.* colorless kernels); (2) transposon-tagged *a1* alleles have been cloned and characterized, *e.g.*, *a1-mum2* and *a1::rdt* alleles (O'Reilly *et al.* 1985; Brown *et al.* 1989a), and a substantial degree of DNA sequence polymorphism exists between these alleles (Xu *et al.* 1995) thereby facilitating the high-resolution mapping of recombination breakpoints; and (3) genetic markers flanking the *a1* locus are available for distinguishing between NCO and CO events.

The *a1* locus was used to test the effects of the *trans*-acting regulatory transposon *MuDR* (Schnable and Peterson 1986; Chomet *et al.* 1991; Hershberger *et al.* 1991; Qin *et al.* 1991; Hsia and Schnable 1996) on the frequency and distribution of intragenic meiotic recombination events in the vicinity of the *Mu1* nonautonomous transposon insertion. Rates of meiotic COs in the vicinity of a *Mu1* insertion increase in the presence of *MuDR*, thereby demonstrating that *MuDR* is active during meiosis. We hypothesize that this stimulation of meiotic COs occurs via the introduction of DNA breaks generated by *MuDR* at the *Mu1* insertion and that these DNA breaks stimulate meiotic COs in plants.

MATERIALS AND METHODS

Genetic stocks: The origins and natures of the recessive *a1-mum2* and *a1::rdt* alleles have been reviewed previously (Xu *et al.* 1995). In summary, the *a1-mum2* allele contains a 1.4-kb *Mu1* transposon insertion at position −97 and the *a1::rdt* allele carries a 0.7-kb *rdt* transposon insertion in the fourth exon. Both of these alleles condition a colorless kernel phenotype in the absence of *trans*-acting regulatory transposons *MuDR* and *Dotted* [*Dt*], respectively. In the presence of *MuDR* or *Dt*, the nonautonomous *Mu1* or *rdt* transposons can excise from *a1*. If this occurs during kernel development a spotted phenotype results. The *shrunken-2* (*sh2*) gene is located on chromosome 3 ~0.1 cM centromere distal from the *a1* locus (Civardi *et al.* 1994). Mutations at this locus condition a shrunken kernel phenotype.

Two stocks were derived from a maize line obtained from D. S. Robertson that carried *a1-mum2* and many genetically active copies of *MuDR*. Sibling spotted and nonspotted kernels derived from the same ears were used as the *a1-mum2* with and without *MuDR* stocks, respectively. Consequently, these stocks differ by only the presence or absence of *MuDR*. The *a1-dl* stock is as described by Xu *et al.* (1995).

Isolation of genetic recombinants: Crosses 1 and 2 were conducted by planting the indicated parents in plots isolated from other maize pollen sources during the summer of 1994.

Cross 1: *a1-mum2 Sh2/a1::rdt sh2* (without *MuDR*) × *a1::rdt sh2/a1::rdt sh2*.
Cross 2: *a1-mum2 Sh2/a1::rdt sh2* (with *MuDR*) × *a1::rdt sh2/a1::rdt sh2*.

The female parents (listed first) were detasseled prior to anthesis to ensure that they would be pollinated by only the *a1::rdt sh2* male parent. As expected, most of the progeny from these crosses had colorless, round (or spotted round when *MuDR* was present; class I, Figure 1) or colorless, shrunken (class II, Figure 1) kernel phenotypes. However, if intragenic recombination occurred in *a1*, four recombinant classes (Figure 1, classes III–VI) could also result; three of these can be identified via their nonparental phenotypes. Class IV recombinants condition a parental phenotype and therefore could not be identified. NCOs initiated from the *a1-mum2 Sh2* chromosome (class VI) would condition colored round kernels. In the current study, this class could not be analyzed due to the difficulty in distinguishing colored kernels from the very heavily spotted kernels that contain *MuDR*. The two remaining recombinant classes (III and V) produce colored, shrunken kernels. These kernels were putative recombinants arising from either COs between the *Mu1* and *rdt* transposon insertion sites in the *a1-mum2* and *a1::rdt* alleles (class III, Figure 1) or gene conversion events in which the *rdt* transposon sequence and its flanking sequences were replaced by the corresponding sequences from the *a1-mum2* allele (class V, Figure 1). In either case, the genotype of these kernels was designated *A1′ sh2/a1::rdt sh2*. To verify and purify the putative recombinant alleles, colored shrunken kernels from crosses 1 and 2 were planted and subjected to cross 3. Colored, round kernels from cross 3 were then planted and the resulting plants were self-pollinated (cross 4).

Cross 3: *A1′ sh2/a1::rdt sh2* × *a1-dl Sh2/a1-dl Sh2*.
Cross 4: *A1′ sh2/a1-dl Sh2* self.

The colored, shrunken kernels resulting from cross 4 were expected to be homozygous for the recombinant chromosome. The two types of recombination events that gave rise to *A1′* alleles (*i.e.*, CO and NCO) were distinguished using two genetic markers that flank the *a1* locus on chromosome 3L (Civardi *et al.* 1994). RFLP marker *php10080* is 2 cM centromere-proximal to the *a1* locus and the phenotypic marker, *sh2*, is 0.09 cM centromere-distal to the *a1* locus.

Generating plasmid clones for sequencing the 3′ regions of *a1-mum2* and *a1::rdt*: Within the 1.2-kb interval defined by the insertion sites of *Mu1* and *rdt*, 20 DNA sequence polymorphisms exist between the *a1-mum2* (GenBank accession no. AF347696) and *a1::rdt* alleles (GenBank accession no. AF072704). To sequence the region proximal to the *rdt* insertion site, the 10-kb *a1::rdt* clone pE10 (Xu *et al.* 1995) was digested with *Sal*I and a 2.6-kb fragment that contains the 3′ region of the *a1::rdt* allele was subcloned into pBKS (Stratagene, La Jolla, CA) to create pSL2.6. Clone pSL2.6 was subsequently digested with *Sac*I or *Kpn*I to generate two overlapping subclones: 1.5-kb pSC1.5 and 1.4-kb pKN1.4, respectively. Clones pSL2.6, pSC1.5, and pKN1.4 were used as templates for sequencing the proximal region of the *a1::rdt* allele. A 1.0-kb fragment resulting from the *Sac*I digestion of the 3.0-kb *a1-mum2* subclone pYEN1 (Xu *et al.* 1995) was subcloned into pBKS to generate pSC1.0. Clones pYEN1 and pSC1.0 were used as templates for sequencing the proximal region of the *a1-mum2* allele.

Oligonucleotides: Because the genic sequence of the *a1-mum2* allele (AF347696) is identical to the *A1-LC* allele (Yao *et al.* 2002), oligonucleotides used as primers for PCR and sequencing were designed from the existing sequence of the *A1-LC* allele (GenBank accession nos. X05068, AF363390, and AF363391). With the exception of the *a1-mum2*-specific primer QZ1543, these oligonucleotides could also amplify the *a1::rdt* allele due to the high degree of sequence identity (98%) between *a1-mum2* and *a1::rdt*.

The sequences of the oligonucleotides used as primers for PCR and sequencing were as follows: QZ1543, 5′ AAA CAT AAA AAC AAT ACG TAA TCC AG 3′ (*a1-mum2*-specific primer); XX907, 5′ GTG TCT AAA ACC CTG GCG CA 3′; QZ1003, 5′ ATA ATA GTA GCC TCC CGA ATA A 3′; XX231, 5′ GCC AAA CTC TGA TTC GCT CCG TG 3′; XX390, 5′ TCG GCT TGA TTA CCT CAT TCT 3′; XX025, 5′ GGT AGG GCA GCG TGT GGT GTT 3′ (Xu *et al.* 1995); and XX026, 5′ GAG GTC GTC GAG GTG GAT GAG CTG 3′ (Xu *et al.* 1995). The positions of the primers within the *a1* gene are illustrated in Figure 2A.

Polymerase chain reaction: PCR was conducted for 40 cycles on a programmable thermal controller (MJ Research, Watertown, MA) as follows: denaturation was conducted at 94° for 1 min, annealing at the indicated temperature for 50 sec, and extension at 72° for 1 min. The annealing temperature varied among primer pairs. The annealing temperature was 3° below the lower of the melting temperatures [2 × (A + T) + 4 × (G + C)] of the two primers used in the PCR reaction. PCR reactions included 0.2 mM dNTP (Pharmacia Biotech, Piscataway, NJ), 1.5 mM $MgCl_2$, 0.5 μM of each primer, and *Taq* polymerase in a total volume of 25 μl. In those instances where nonspecific bands amplified, "hot start" PCR was utilized (Newton *et al.* 1989; Chou *et al.* 1992).

Mapping the breakpoints of COs and the distal (5′) endpoints of conversion tracts relative to a diagnostic *Pst*I site: On the basis of the strategy used to select recombinants, the breakpoints of all COs and the distal endpoints of all conversion tracts of NCOs recovered in this experiment were expected to fall within the 1.2-kb interval defined by the *Mu1* and *rdt* insertion sites in each of the parental *a1* alleles (Figure 2A). Previously, Xu *et al.* (1995) identified a diagnostic *Pst*I site within this 1.2-kb interval that can distinguish between *a1-mum2* and *a1::rdt* derived sequences. This site is present in the *a1::rdt* allele, but absent from the *a1-mum2* allele. Thus, *Pst*I digestion of PCR-amplified recombinant alleles can be used to map the position of the breakpoint of each CO or the distal endpoint of each gene conversion tract relative to this site.

Primers (XX025 and XX026) were used to PCR amplify this 1.2-kb interval from each recombinant allele (Figure 2A). The 1.2-kb PCR products were fractionated by electrophoresis, purified by binding to NA45 DEAE membrane (Schleicher & Schuell, Keene, NH), and subjected to *Pst*I digestion. If a given PCR product was digested by *Pst*I, the breakpoint of the CO or the distal endpoint of the conversion tract associated with the corresponding *A1′* allele did not extend 5′ of this diagnostic *Pst*I site. Alternatively, if the PCR product was resistant to *Pst*I digestion, the breakpoint of the CO or the distal endpoint of the conversion tract was between the diagnostic *Pst*I site and the *Mu1* insertion site. Thirty-six of the 40 *A1′* alleles were successfully amplified and mapped relative to the diagnostic *Pst*I site.

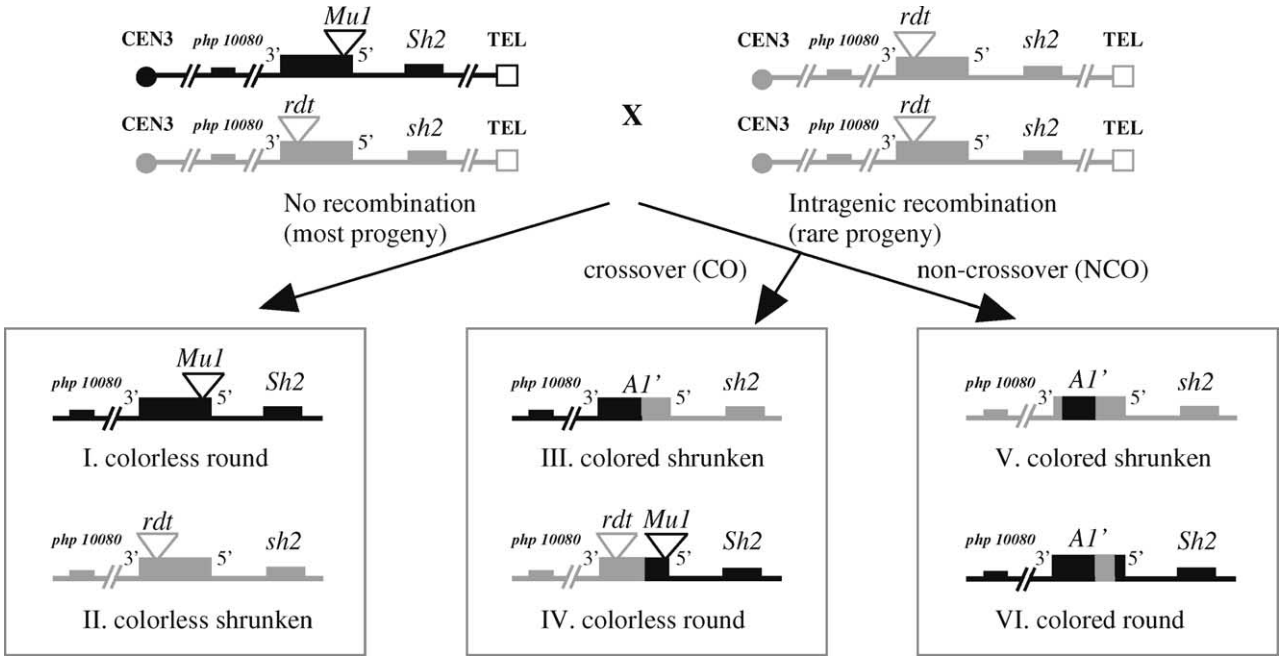

FIGURE 1.—Isolation of intragenic recombinant *A1′* alleles. The parents of and the progeny resulting from crosses 1–2 are illustrated. Chromosomes from the *a1-mum2* and *a1::rdt sh2* stocks are illustrated in black and gray, respectively. The RFLP marker *php10080* and the *a1* and *sh2* genes are represented by black (if derived from *a1-mum2* chromosome) or gray (if derived from *a1::rdt* chromosome) boxes. Triangles indicate the positions of *Mu1* and *rdt* transposon insertions in the *a1* gene. Class III and IV COs arise following DNA breaks on either chromosome. Class V and VI NCOs arise following breaks on the *a1::rdt*- and *a1-mum2*-containing chromosomes, respectively. Only the colored shrunken recombinants (classes III and V) were characterized in this study. Class I progeny will be spotted if they carry *MuDR*.

PCR-based sequencing of the recombinant *A1′* alleles: Once a CO breakpoint or conversion tract endpoint was mapped relative to the diagnostic *Pst*I site, the region of the corresponding *A1′* allele that contained the recombination endpoint was PCR amplified, purified, and sequenced. Purified PCR products amplified using primers XX025 and XX026 from each of the 36 *A1′* alleles were used as templates for sequencing. For those 30 alleles that had breakpoints or endpoints distal to the polymorphic *Pst*I site, primers XX390 and XX025 were used for sequencing. For those 6 alleles with breakpoints or endpoints proximal to the polymorphic *Pst*I site, primers XX231 and XX026 were used for sequencing (Figure 2A). The positions of each CO breakpoint and the conversion tract endpoints proximal or distal to the polymorphic *Pst*I site were identified by comparing the DNA sequence polymorphisms present in a given recombinant *A1′* allele to those in *a1-mum2* and *a1::rdt*.

RESULTS

Isolation of recombination events: Intragenic recombination events were isolated at the *a1* locus as illustrated in Figure 1. The *a1-mum2* and *a1::rdt* alleles used in these crosses both condition a colorless kernel phenotype in the absence of *MuDR* and *Dt*, due to resident *Mu1* and *rdt* transposon insertions, respectively. Therefore, most of the progeny from these crosses had a colorless (or spotted in the presence of *MuDR*) kernel phenotype and genotypes of either *a1-mum2 Sh2/a1::rdt sh2* or *a1:rdt sh2/a1::rdt sh2*. However, colored kernels were recovered in rare cases as a result of intragenic recombination that led to the generation of chimeric alleles with restored *a1* gene function. These functional recombinant alleles were designated *A1′*.

To test the effect of the *trans*-acting regulatory element *MuDR* on CO frequency, colored shrunken kernels (Figure 1, classes III and V) were selected from parallel crosses without (cross 1) and with (cross 2) *MuDR*. The colored round class (class VI) was not analyzed for two reasons. First, a previous *Mu* transposition study in *a1* (LISCH *et al.* 1995) demonstrated that *Mu1* excision and repair from *a1-mum2* generates fully restored alleles at a low rate, $<10^{-4}$. Second, coupled with the extremely low rate of reversion at *a1-mum2*, it is very difficult to distinguish the colored round class (class VI) from the very heavily spotted parental phenotype obtained from cross 2.

Recombinant *A1′* alleles isolated from crosses 1 and 2 that were in coupling with the closely linked *sh2* mutant allele could have arisen via either COs that resolved between the *Mu1* and *rdt* insertion sites or NCOs having conversion tracts that span the *rdt* transposon insertion site. These putative colored shrunken recombinants were analyzed as described in MATERIALS AND METHODS. The validity of 8 cross 1 and 32 cross 2 recombinants were confirmed via testcrosses and/or RFLP analysis (Table 1) using marker *php10080* as described by XU *et al.* (1995).

Two genetic markers (*php10080* and *sh2*) that flank

TABLE 1

Number of recombinant *A1′* alleles isolated

	No. colored shrunken kernels isolated	% confirmed by testcross[a]	No. confirmed by RFLP analyses[b]			Corrected no.[c]		
			CO + NCO	CO	NCO	CO + NCO	CO	NCO
Cross 1, without *MuDR*	17	100	8	5	3	17	11	6
Cross 2, with *MuDR*	58	82	32	27	5	47	40	7

[a] Because not all putative recombinants were successfully testcrossed, corrected numbers of recombinants were calculated (see footnote *c*).

[b] The positions of the 32 CO breakpoints and of the eight NCO conversion tract endpoints are provided in the APPENDIX.

[c] Because not all of the colored shrunken recombinants were classified as COs or NCOs by genetic testcrosses and RFLP analyses, the numbers of CO and NCO events were estimated using the following formulas:

$$\text{Corrected no. of COs} = \text{total colored, shrunken kernels isolated (}i.e.\text{, all putative recombinants)} \times \%\ \text{confirmed} \times [\text{confirmed no. of CO}/(\text{confirmed no. of CO} + \text{confirmed no. of NCO})].$$

$$\text{Corrected no. of NCOs} = \text{total colored, shrunken kernels isolated (}i.e.\text{, all putative recombinants)} \times \%\ \text{confirmed} \times [(\text{confirmed no. of NCO}/(\text{confirmed no. of CO} + \text{confirmed no. of NCO})].$$

Homogeneity χ^2 values for the rates of CO and NCO were calculated on the basis of the corrected number of COs and NCOs (see footnote *b* in Table 2).

the *a1* locus were used to distinguish between COs and NCOs. Of the 40 recombinants analyzed with these markers, 32 events displayed nonparental markers and therefore arose via COs; the remaining 8 exhibited parental flanking markers and were therefore determined to have arisen via NCOs (Table 1).

The rates of recombination at the *a1* locus in the presence or absence of *MuDR* are shown in Table 2. The genetic distances (CO + NCO) associated with the 1.2-kb interval derived from cross 1 (without *MuDR*) and cross 2 (with *MuDR*) are significantly different (0.008 *vs.* 0.02 cM). Although the rate of class V NCOs was unaffected by the presence of *MuDR*, the rate of CO was four times higher in the presence of *MuDR* than in its absence (0.02 *vs.* 0.005 cM). On the basis of the DSB repair model, NCOs analyzed in this study (class V) must have been initiated by DNA breaks on the *a1::rdt*-containing homolog. Consistent with *MuDR*'s ability to interact with *Mu1* but not *rdt*, the rate of the class V NCOs was unaffected by the presence (cross 2) or absence (cross 1) of *MuDR*. Class VI events (NCOs initiated from *a1-mum2*; Figure 1) would be colored and round. Because such kernels can be extremely difficult to distinguish from heavily spotted *a1-mum2* kernels, and no germinal revertants of *a1-mum2* were identified in a previous screen of 10,000 kernels (LISCH *et al.* 1995), the rates at which class VI events occur were not initially determined in this study. We subsequently attempted

TABLE 2

Rates of intragenic recombination at the *a1* locus

	Corrected no.			Population size	Rates (cM)[a]			CO/NCO[c]
	CO + NCO	CO	NCO		CO + NCO	CO[b]	NCO	
Cross 1, without *MuDR*	17	11	6	408,000	0.008 ± 0.001	0.005 ± 0.001	0.003 ± 0.0009	1.8
Cross 2, with *MuDR*	47	40	7	530,800	0.02 ± 0.002	0.02 ± 0.002	0.003 ± 0.0008	5.7

[a] Because only two of the four possible classes of recombination events were analyzed (III and V in Figure 1), the genetic distance associated with the 1.2-kb interval defined by the *Mu1* and *rdt* insertion sites was calculated by doubling the rate of the corrected number of recombinants analyzed (see footnote *c* in Table 1). This calculation is based on the assumption that the frequencies of class III and IV CO events are equal and that the frequencies of class V and VI NCO events are equal. Because COs are reciprocal events it is reasonable to assume that the rates of class III and IV CO events are equal. Although it is not necessarily true that the rates of class V and VI NCOs are equal, the rate of class V events was doubled to allow comparisons between rates of COs and NCOs. Although the rates presented in this table cannot be used to draw conclusions regarding the rates of class VI NCOs, on the basis of a separate experiment, the rate of class VI NCOs in the presence of *MuDR* is low ($\sim 10^{-5}$).

[b] The homogeneity χ^2 value for the rates of CO with and without *MuDR* ($\chi^2 = 9.9$, $P = 0.002$) indicated that the difference between these rates is significant. In contrast, the homogeneity χ^2 test showed no significant difference between the rates of the NCO from cross 1 and cross 2 ($\chi^2 = 0.04$, $P = 0.84$).

[c] CO/NCO ratios were calculated using only class III COs and class V NCOs (see footnote *a*).

to isolate class VI events from the *a1-mum2* source used in this study to determine the frequency at which *MuDR*-induced DNA breaks are repaired via conversion. Round kernels that appeared to be fully colored and that carried *a1-s* were selected from the progeny of *a1-mum2 Sh2/a1 sh2* plants that carried *MuDR* and that had been crossed by an *a1-s* pollen source (a cross similar to cross 2). Only one excision event was confirmed from a population of ~46,000 spotted kernels (data not shown). Therefore, the rate of reversion of *a1-mum2* to *A1′* (class VI events), *i.e.*, $\sim 10^{-5}$, did not differ significantly from the rates of NCO from the *a1::rdt* chromosome (class V events) in the presence or absence of *MuDR* (Table 2). Hence, the increased rate of recombination that occurs in the presence of *MuDR* is due to an increased rate of COs.

Physical mapping of recombination breakpoints of COs and the 5′ (distal) endpoints of conversion tracts: The conversion endpoints of 8 NCO events and the recombination breakpoints of 28 CO events were physically mapped. Because recombinants were selected on the basis of their colored, shrunken phenotypes, the breakpoints of all the COs and the distal endpoints of the conversion tracts must have resolved within the 1.2-kb interval defined by the *Mu1* and *rdt* transposon insertion sites (Figure 2).

Digestion with *Pst*I revealed that the distal endpoints of six of the eight conversion tracts map 5′ of the diagnostic *Pst*I site that is polymorphic between *a1-mum2* and *a1::rdt*. By virtue of the selection scheme used in the experiment, the conversion tracts cannot contain *Mu1*. Hence, the distal endpoints of these six conversion tracts must lie between the *Pst*I site and the *Mu1* insertion site. The 1.2-kb interval between the *Mu1* and *rdt* insertion sites exhibits 20 polymorphisms between the *a1-mum2* (GenBank accession no. AF347696) and *a1::rdt* alleles (GenBank accession no. AF072704). Regions containing the CO breakpoints or conversion tract endpoints associated with each of 36 *A1′* alleles were PCR amplified and the purified PCR products were sequenced. The sequence derived from each recombinant *A1′* allele was then compared to the sequences of the *a1-mum2* and *a1::rdt* alleles. The switchpoint of sequence polymorphisms within each recombinant allele established, at the highest possible resolution, the position of each CO breakpoint or NCO conversion tract endpoint. The distributions of the CO breakpoints and the distal endpoints of the NCO conversion tracts are illustrated in Figure 2B. Whereas recombination hotspots in yeast are defined by regions of high DSB frequency, recombination hotspots in this and other plant studies are defined as regions with elevated rates of recombination resolution endpoints. The distal endpoints of 6 of 8 NCO events and the CO breakpoints of 21 of 28 crossover events mapped to the previously defined 377-bp recombination hotspot at the 5′ end of the *a1* coding sequence (Xu *et al.* 1995).

Physical mapping of the 3′ (proximal) endpoints of conversion tracts: On the basis of the genetic screen used to isolate recombination events, we believe that the proximal endpoints for all of the conversion tracts must have resolved proximal to the *rdt* insertion site. Only two DNA sequence polymorphisms exist between the *a1-mum2* and *a1::rdt* alleles in the 1.6 kb proximal to the *rdt* insertion site (Figure 2A). One of these polymorphisms is a 32-bp insertion/deletion that is present in the *a1-mum2* allele, but absent from the *a1::rdt* allele. By using an *a1-mum2*-specific primer (QZ1543) that anneals to the 32-bp polymorphic sequence in combination with a primer (XX907) that amplifies both *a1-mum2* and *a1::rdt* alleles, it was possible to map the proximal endpoints of the conversion tracts relative to this 32-bp polymorphic site (Figure 2C). The ability of these primers to PCR amplify a given *A1′* allele indicated that the conversion tract contained the 32-bp polymorphic sequence. Such a result would indicate that the proximal conversion tract endpoint was proximal to the 32-bp polymorphic site. The proximal conversion tract endpoints of four *A1′* alleles derived from NCOs mapped proximal to the 32-bp polymorphic site. The 1059 bp proximal to this polymorphism are identical between the two *a1* alleles. No *a1*-specific RFLPs were detected between *a1-mum2* and *a1::rdt* that mapped between the 32-bp polymorphism and *php10080* when the 1.0-kb *Sac*I/*Eco*RI fragment from the *a1-mum2* subclone pSC1.0 was used as a hybridization probe in a DNA gel blot experiment involving genomic DNA (data not shown). As a result, the proximal endpoints of these four conversion tracts could not be determined with higher precision.

A negative PCR result using primers QZ1543 and XX907 demonstrated that the proximal endpoint of an NCO was distal to the 32-bp polymorphic site. The proximal endpoints of four NCO *A1′* alleles mapped distal to the 32-bp polymorphism. To map these proximal endpoints to higher resolution, the corresponding *A1′* alleles were PCR amplified using primers XX907 and QZ1003 (Figure 2A). By comparing the sequences of the resulting 0.9-kb PCR product to the *a1* parental alleles used to generate the *A1′* alleles, the proximal endpoints were mapped at the highest possible resolution afforded by the sequence polymorphisms present between the parental alleles. The proximal endpoints of all four of these conversion tracts mapped to interval XXIII (Figure 2C). Although three of the conversion tracts are indistinguishable, they must have arisen via independent events because they were recovered from separate female parents in crosses 1 and 2.

Lengths of conversion tracts: Because the positions of both the distal and the proximal endpoints of four conversion events were established, it was possible to

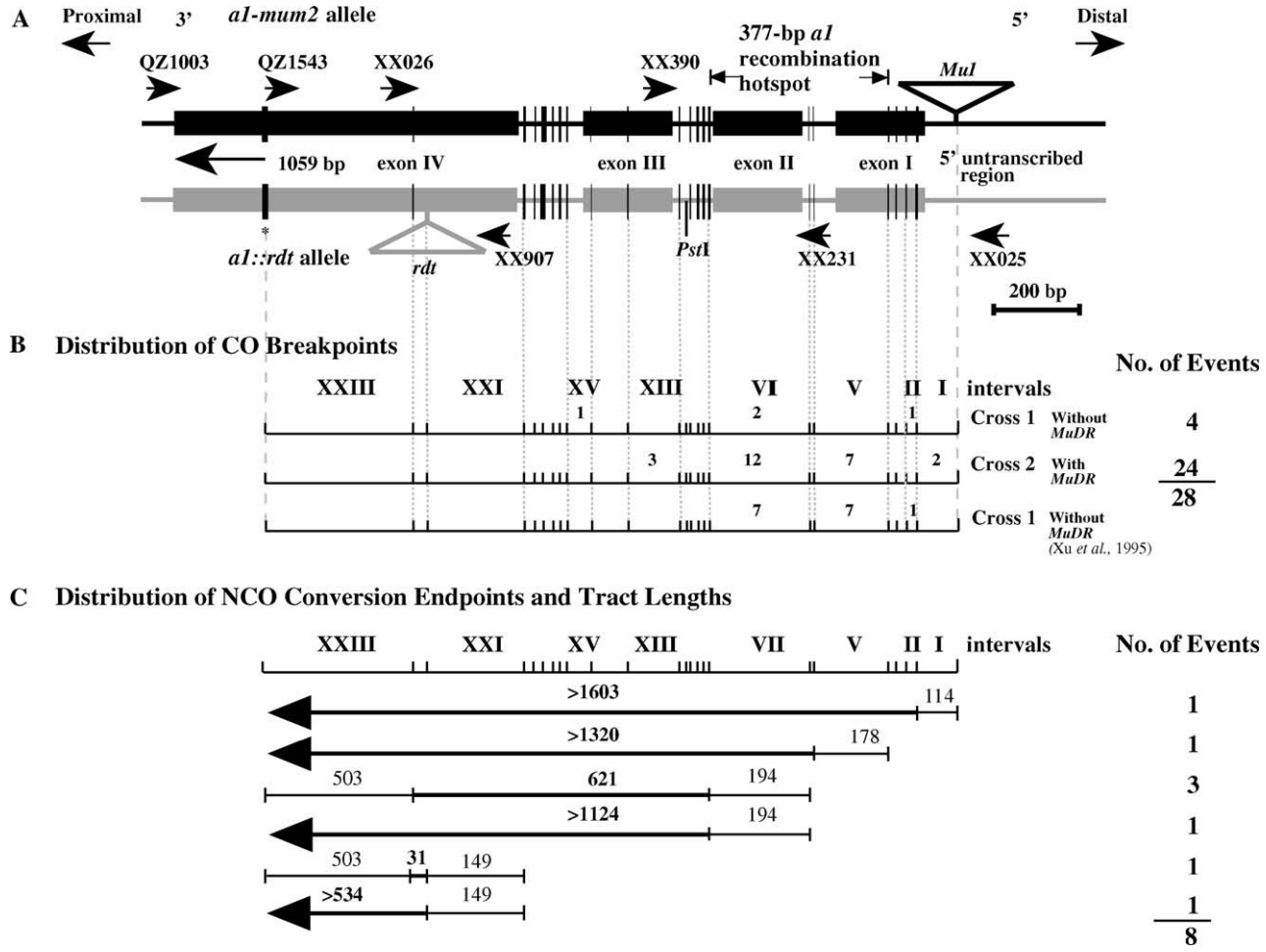

FIGURE 2.—Physical mapping of CO breakpoints and NCO conversion tracts. (A) Schematic of the *a1-mum2* and *a1::rdt* alleles in which boxes and triangles represent exons and transposon insertions, respectively. The RFLP marker *php10080* and the *sh2* locus are proximal and distal to the *a1* locus, respectively. The positions of primers used for PCR amplification and sequencing and the diagnostic *Pst*I site are indicated. The *a1* gene is separated into 23 intervals defined by the 24 polymorphisms (vertical lines) between the *a1::rdt* and *a1-mum2* alleles. The width of a given vertical bar is proportional to the number of base pairs involved in the polymorphism. The 3′-most polymorphic site (a 32-bp insertion/deletion) is indicated by an asterisk. Sequences 1059 bp 3′ of this site are identical between the *a1::rdt* and *a1-mum2* alleles. (B) Locations of CO recombination breakpoints associated with *A1′* alleles. Intervals are defined by the polymorphic sites shown in A. The numbers of recombination breakpoints that resolved in each interval are indicated. The 377-bp recombination hotspot identified previously (XU *et al.* 1995) is indicated. Data from XU *et al.* (1995) are provided for reference. (C) Locations of NCO conversion endpoints and sizes of conversion tracts associated with eight *A1′* alleles isolated from crosses 1 and 2. When possible, conversion tract endpoints were mapped relative to pairs of DNA sequence polymorphisms. Sequences confirmed to be included in the conversion tract are measured in base pairs above the bold lines. Conversion tract endpoints can be positioned relative to the nearest polymorphism and the size of the tract is equal to or less than the length of the thin line. The proximal ends of four conversion tracts (arrows on left side of bold lines) lie to the proximal side of the polymorphic site indicated by an asterisk in A. The numbers of *A1′* alleles with the indicated type of conversion tract are indicated on the right.

calculate the sizes of the conversion tracts associated with each of the resulting *A1′* alleles. As depicted in Figure 2C, three of the four conversion tracts were between 621 and 1318 bp in length. The fourth is between 31 and 683 bp. For the remaining four conversion events, although their distal endpoints were mapped at the highest possible precision, it was not possible to map their proximal endpoints because of a lack of polymorphisms between the parental *a1* alleles (*a1-mum2* and *a1::rdt*). Therefore, the absolute sizes of these four conversion tracts could not be determined. However, on the basis of the positions of the corresponding distal endpoints, the lengths of these conversion tracts must be in excess of 534 bp (1 allele), 1124 bp (1 allele), 1320 bp (1 allele), and 1603 bp (1 allele).

DISCUSSION

Physical characterization of NCO conversion tracts: The average lengths of meiotic conversion tracts at the

rosy locus of *Drosophila melanogaster* (Hilliker *et al.* 1994) and the *rp49* locus of *D. subobscura* (Betran *et al.* 1997) are 352 and 122 bp, respectively. In contrast, the average tract lengths associated with Drosophila *P*-element excision were somewhat larger, *i.e.*, ~1400 bp (Gloor *et al.* 1991; Preston and Engels 1996). In yeast, the average meiotic conversion tract lengths range from 0.4 to 1.6 kb in a 9-kb interval (Borts and Haber 1989). Even so, longer conversion tracts of 9 and 12 kb have also been observed in yeast (Borts *et al.* 2000). Conversion tracts >5 kb have also been observed in Neurospora (Yeadon and Catcheside 1998). Few plant conversion tracts have been characterized. In maize, two *a1* conversion tracts were in excess of 621 and 815 bp (Xu *et al.* 1995) and two *bz1* conversion tracts were between 965 and 1165 bp and between 1.1 and 1.5 kb (Dooner and Martinez-Ferez 1997b). The conversion tracts of two NCO-like events isolated from the maize *Kn1-O* tandem duplication (Mathern and Hake 1997) are 1.7 and 3 kb. Yao *et al.* (2002) identified two putative NCOs from the maize *a1-sh2* interval that have conversion tracts that are at least 17 kb.

The eight conversion tracts characterized in this study (crosses 1 and 2) ranged in size from >31 bp to >1603 bp. These NCO events resulted from conversion of the *rdt* insertion and its surrounding sequences and were therefore initiated by DSBs on the *a1::rdt*-containing chromosome. Conversion tracts on the *a1::rdt*-containing chromosome that extended 5′ of the *Mu1* insertion site would not have been recovered.

The single revertant allele isolated from *a1-mum2* in this study exhibited 100% identity to the wild-type progenitor of *a1-mum2* (*i.e.*, *A1-LC*). This revertant may therefore have arisen via a class VI NCO event (Figure 1) within the interval 51 bp upstream and 165 bp downstream of the *Mu1* insertion site that lacks polymorphisms between the parental alleles of crosses 1 and 2. This would be consistent with the finding that in mice and yeast, gene conversion tracts can be <100 bp (Sweetser *et al.* 1994; Elliott *et al.* 1998; Palmer *et al.* 2003).

Factors affecting CO/NCO ratios: In yeast heterozygotes, the presence of only a few nucleotide polymorphisms can drastically affect the frequencies at which COs (Borts and Haber 1987; Borts *et al.* 1990) and NCOs (Chen and Jinks-Robertson 1999; Nickoloff *et al.* 1999) are recovered. For example, 0.09% heterology between alleles at the *MAT* loci in yeast reduced COs by twofold and increased the rate of NCOs by threefold (Borts *et al.* 1990). Similarly, in the maize *bz1* gene, the degree of sequence similarity between the parental alleles affects the CO/NCO ratio (Dooner 2002). In Dooner's study the CO/NCO ratio observed between *bz1* "heteroalleles" was >20. In the current study, the CO/NCO ratio observed in plants that lacked *MuDR* was 1.8. This dramatic difference in the CO/NCO ratio between the two studies cannot be attributed to differences in the degree of DNA sequence polymorphism, because Dooner's heteroalleles exhibited approximately the same degree of DNA sequence polymorphism (1.5%) as the parental *a1* alleles used in the current study (1.8%). Instead, the ~10-fold difference in the CO/NCO ratios between the two studies could be a consequence of locus-specific differences in the relative rates of conversions and crossovers or differences caused by genetic background. Although it is not possible to exclude locus-specific effects, this study does establish that CO/NCO ratios can be influenced by the differences in genetic background. Specifically, this study establishes that *MuDR* affects CO/NCO ratios. For example, the CO/NCO ratios differ by more than threefold between crosses 1 and 2 (compare CO/NCO ratios, Table 2) for which the genetic backgrounds are identical except for the absence (cross 1) or presence (cross 2) of *MuDR*. We cannot exclude the possibility that the relative impacts of *MuDR* on rates of COs and NCOs may differ depending upon the level of sequence heterology present in a heterozygote. For example, it is possible that in heterozygotes exhibiting a degree of heterology lower than that present in crosses 1 and 2, *MuDR* might increase the rate of NCOs. This, however, seems unlikely given that reversions of *Mu*-induced alleles of all loci studied are quite rare in diverse genetic backgrounds, which would be expected to exhibit varying levels of heterology at the target loci.

***MuDR* increases the rate of COs at *a1*:** According to the most widely accepted recombination models (Szostak *et al.* 1983; Sun *et al.* 1991; Allers and Lichten 2001), which are well supported by data from yeast, meiotic recombination is initiated by DSBs and the subsequent repair and resolution of these DSBs results in COs or NCOs. Although in plants the mechanisms underlying meiotic recombination are not as well understood, it is thought that they are at least similar to those that occur in yeast. Support for this view comes from the isolation of plant homologs of many of the yeast genes involved in DSB processing and meiotic recombination (reviewed in Bhatt *et al.* 2001; Schwarzacher 2003). Also, agents that introduce DSBs into plant chromosomes increase rates of mitotic recombination and intrachromosomal recombination.

It has not yet, however, been determined in plants whether the stimulation of DNA breaks increases the rate of homologous meiotic recombination. To address this question, recombinants were isolated from *a1-mum2/a1::rdt* heterozygotes that carried or did not carry *MuDR*. *MuDR* encodes a transposase (Chomet *et al.* 1991; Hershberger *et al.* 1991; Qin *et al.* 1991; Hsia and Schnable 1996) required for the transposition of *Mu* elements. This transposition must involve some type of DNA breaks. The recovery of chromosomes that contain deletions of sequences adjacent to *Mu* elements and internally deleted *Mu* elements is consistent with the existence of *MuDR*-catalyzed DNA breaks in the

vicinity of *Mu* elements (Levy *et al.* 1989; Levy and Walbot 1991; Lisch *et al.* 1995; Hsia and Schnable 1996; Asakura *et al.* 2002; Kim and Walbot 2003). Because the mechanism by which *MuDR* catalyzes transposition has not been determined, these *MuDR*-generated breaks could be either DSBs or single-strand nicks. It has long been assumed that these breaks were DSBs, but recent evidence suggests that single-strand nicks can stimulate homologous recombination in the V(D)J regions of immunoglobulin genes (Lee *et al.* 2004). Hence, *MuDR*-generated single-strand nicks could affect recombination directly or could be converted into DSBs during DNA replication (Kuzminov 2001). Alternatively, *MuDR* may directly catalyze DSB formation.

Regardless of the mechanism by which *MuDR* generates DNA breaks, crosses harboring *MuDR* would be expected to have an increased rate of breaks in the vicinity of the *Mu1* insertion in the *a1-mum2* allele. At least three processes could repair *MuDR*-induced DNA breaks at *a1-mum2*. These include COs between the two homologs (class III and IV events, Figure 1); conversion of the *Mu1*-containing homolog, using as template the homolog that does not contain *Mu1* (class VI NCO events, Figure 1); or DSB repair, using as template the sister chromatid. This latter process would not generate recombinant chromosomes and would in fact regenerate the parental *a1-mum2* allele or either internal or adjacent deletions of *Mu1* if gap repair is interrupted (Lisch *et al.* 1995; Hsia and Schnable 1996; Asakura *et al.* 2002; Kim and Walbot 2003).

MuDR is required for the transposition of *Mu* transposons, a process that requires the introduction of DNA breaks. According to accepted recombination models, COs are also initiated by DNA breaks. Hence, we interpret our observation that plants that carry *MuDR* exhibit four times more class III COs (Figure 1) than do plants that do not carry *MuDR* (Table 2) to indicate that during meiosis at least some *MuDR*-induced DNA breaks are repaired via the CO pathway. Hence, our results strongly suggest that DNA breaks stimulate meiotic COs in plants.

Although *MuDR* stimulates meiotic COs, the *Ac* transposon does not (Dooner and Martinez-Ferez 1997a). This suggests that *Ac*-induced DSBs are separated temporally or spatially from meiotic recombination (Dooner and Martinez-Ferez 1997a) or that *Ac*-induced DSBs are repaired by another pathway, for example via the formation of hairpins followed by nonhomologous end joining (NHEJ) repair at sites of microhomology (Weil and Kunze 2000; Yu *et al.* 2004).

We cannot rule out the possibility that the increased rates of CO observed in this study are not a direct consequence of an increased rate of breaks at *Mu1* but are instead a consequence of potential changes in the chromatin architecture at *a1-mum2* that occur in the presence of *MuDR*. Even if the transposase *per se* is not generating breaks at the *Mu1* insertion site, the transposase must at least be creating a local environment that is more conducive to the formation of endogenous DNA breaks. If this alternative model is correct, a *MuDR*-encoded transposase that can bind to *Mu* terminal inverted repeats, but that cannot catalyze transposition, should increase the rate of recombination in the vicinity of a *Mu* insertion. Regardless of whether the breaks are caused directly or indirectly by *MuDR*, it is clear that *MuDR* stimulates the formation of DNA breaks at the *a1-mum2* allele, resulting in increased rates of meiotic CO.

Does *MuDR* affect the rate of gene conversion? There are two classes of NCOs (classes V and VI, Figure 1). Although *MuDR* increased the rate of COs it did not increase the rate of class V NCOs in the *a1-mum2/a1::rdt* heterozygote. This is as expected because *MuDR* would not be predicted to interact with *a1::rdt*. In contrast, the existence of somatic excision events in *MuDR*-containing stocks demonstrates that *MuDR* interacts (directly or indirectly) with *Mu* insertions. Even so, germinal reverants of *Mu*-insertion alleles (including class VI NCOs) are rare (reviewed in Bennetzen 1996; Lisch 2002; Walbot and Rudenko 2002); the frequencies of germinal revertants from the *bronze* locus are 8×10^{-5} (Brown *et al.* 1989b) and between 4.9×10^{-6} and 2.3×10^{-3} (Schnable *et al.* 1989). Consistent with these results, we and others (Lisch *et al.* 1995) have shown that the rate of class VI NCOs at *a1-mum2* is low. It is puzzling that in this heterozygote, although *MuDR* increases the rate of CO fourfold, the rate of class VI NCOs is low in the presence of *MuDR*.

In yeast, several meiotic mutants that affect SEI and DHJ formation drastically reduce the frequency of COs but not NCOs. This suggests that recombination outcomes (CO *vs.* NCO repair) are determined prior to stable strand exchange (*i.e.*, SEI; Borner *et al.* 2004). If this is also true in plants, the *MuDR*-generated breaks might be designated prior to strand exchange to be repaired by the CO pathway. In V(D)J site-specific recombination, the RAG recombinases act as molecular shepherds that allow repair of the RAG-generated DSB by the NHEJ machinery and not other repair pathways (Lee *et al.* 2004). Similarly, during meiosis the *MuDR* transposase and/or protein(s) involved in the meiotic recombination machinery may remain bound to the *MuDR*-generated DNA breaks and thereby channel repairs to the CO pathway. It is also possible that some repairs of *MuDR*-induced DNA breaks could be channeled to pathways that were not detected in this study because they do not yield COs or germinal revertants (*e.g.*, repair using the sister chromatid as template or NHEJ). The high somatic and low germinal reversion rates observed in the *Mu* system could be explained if these "molecular shepherds" differ between the mitotic and meiotic cellular programs.

***MuDR* does not affect the distribution of recombination breakpoints:** Insertion/deletion polymorphisms

(IDPs) and transposon insertions suppress recombination in nearby regions of the *bz1* locus (Dooner and Martinez-Ferez 1997b). By doing so these IDPs change the distribution of recombination breakpoints across the *bz1* locus, creating apparent recombination hotspots. In contrast, the distribution of recombination breakpoints across the *a1* gene is not affected by the *Mu1* insertion at position −97 in *a1-mum2* (Xu *et al.* 1995; Yao *et al.* 2002). Hence, the recombination hotspot reported by Xu *et al.* (1995) is not a consequence of the *Mu1* insertion in one of the parental alleles used by that study.

Although the rates of CO at *a1* increase fourfold in the presence of *MuDR*, the distribution of recombination breakpoints is not altered by *MuDR*; 19 of the 24 characterized breakpoints cluster in the 377-bp hotspot at the 5′ end of the *a1* gene (Figure 2B) previously identified in stocks that lack *MuDR* (Xu *et al.* 1995). Hence, the COs that are apparently initiated by *MuDR*-induced breaks at the *Mu1* insertion at −97 resolve at the same positions within *a1* as do the COs that are initiated by the DSBs that form in the absence of *MuDR*. COs resolve in this same hotspot even in an *A1* allele that does not contain a *Mu1* insertion (Yao *et al.* 2002). These findings are consistent with the hypothesis that the DSBs that initiate recombination in nonmutant *a1* alleles occur in the vicinity of position −97. Even though the relationship between the positions of DSB hotspots and recombination hotspots has not yet been studied in plants, the observation that most *a1* recombinants mapped within 700 bp of the *Mu1* insertion site is consistent with the observation that most recombination hotspots in budding yeast are located within 1 or 2 kb of a DSB hotspot (Smith 2001).

***MuDR* is active in meiotic cells:** Although the *Mu* transposase *mudrA* and *mudrB* transcripts are highly expressed in mature pollen and *mudrB* promoter::reporter constructs are expressed at levels 20-fold higher in pollen than in leaves (Raizada *et al.* 2001a), to date, there has not been conclusive evidence that the *MuDR* transposase is active and functions during meiosis. Instead, germinally transmissible *Mu* insertions could arise via late somatic excision in premeiotic cells (reviewed in Walbot and Rudenko 2002) or via postmeiotic transposition (Robertson and Stinard 1993). In contrast, by demonstrating that *MuDR* increases rates of meiotic recombination at *a1-mum2* fourfold, the current study provides the first direct evidence that *MuDR* is active during meiosis.

Evolutionary implications: This study extends our understanding of how transposons can alter recombination rates. The insertion of a nonautonomous transposon into a gene typically reduces the rate of intragenic recombination. For example, the insertion of a *Mu1* transposon into the *A1-LC* allele (which generated *a1-mum2*) reduced the rate of recombination approximately twofold (Xu *et al.* 1995). In contrast and as revealed by this study, if a *Mu*-insertion allele is present in a genome that contains an active copy of *MuDR*, the rate of intragenic recombination can actually be higher (twofold in this case) than that of the original allele that lacked a transposon insertion. Because a variety of plant DNA transposons have an affinity for inserting into genes (Bureau *et al.* 1996; Raizada *et al.* 2001b; Jiang *et al.* 2004) and intragenic recombination can generate new alleles, their ability to alter rates of intragenic recombination could have significant evolutionary implications.

This research was supported in part by competitive grants from the United States Department of Agriculture National Research Initiative Program to P.S.S. and B.J.N. (9701407 and 9901579) and to P.S.S. (0101869 and 0300940). This is journal paper no. J-19273 of the Iowa Agriculture and Home Economics Experiment Station, Ames, Iowa, project nos. 3334, 3485, and 6502, supported by Hatch Act and State of Iowa funds.

LITERATURE CITED

Allers, T., and M. Lichten, 2001 Differential timing and control of noncrossover and crossover recombination during meiosis. Cell **106:** 47–57.

Asakura, N., C. Nakamura, T. Ishii, Y. Kasai and S. Yoshida, 2002 A transcriptionally active maize MuDR-like transposable element in rice and its relatives. Mol. Genet. Genomics **268:** 321–330.

Athma, P., and T. Peterson, 1991 Ac induces homologous recombination at the maize P locus. Genetics **128:** 163–173.

Bennetzen, J. L., 1996 The Mutator transposable element system of maize. Curr. Top. Microbiol. Immunol. **204:** 195–229.

Betran, E., J. Rozas, A. Navarro and A. Barbadilla, 1997 The estimation of the number and the length distribution of gene conversion tracts from population DNA sequence data. Genetics **146:** 89–99.

Bhatt, A. M., C. Canales and H. G. Dickinson, 2001 Plant meiosis: the means to 1N. Trends Plant Sci. **6:** 114–121.

Borner, G. V., N. Kleckner and N. Hunter, 2004 Crossover/noncrossover differentiation, synaptonemal complex formation, and regulatory surveillance at the leptotene/zygotene transition of meiosis. Cell **117:** 29–45.

Borts, R. H., and J. E. Haber, 1987 Meiotic recombination in yeast: alteration by multiple heterozygosities. Science **237:** 1459–1465.

Borts, R. H., and J. E. Haber, 1989 Length and distribution of meiotic gene conversion tracts and crossovers in *Saccharomyces cerevisiae*. Genetics **123:** 69–80.

Borts, R. H., W. Y. Leung, W. Kramer, B. Kramer, M. Williamson *et al.*, 1990 Mismatch repair-induced meiotic recombination requires the pms1 gene product. Genetics **124:** 573–584.

Borts, R. H., S. R. Chambers and M. F. Abdullah, 2000 The many faces of mismatch repair in meiosis. Mutat. Res. **451:** 129–150.

Brown, J. J., M. G. Mattes, C. O'Reilly and N. S. Shepherd, 1989a Molecular characterization of rDt, a maize transposon of the "Dotted" controlling element system. Mol. Gen. Genet. **215:** 239–244.

Brown, W. E., D. S. Robertson and J. L. Bennetzen, 1989b Molecular analysis of multiple *Mutator*-derived alleles of the *Bronze* locus of maize. Genetics **122:** 439–445.

Bureau, T. E., P. C. Ronald and S. R. Wessler, 1996 A computer-based systematic survey reveals the predominance of small inverted-repeat elements in wild-type rice genes. Proc. Natl. Acad. Sci. USA **93:** 8524–8529.

Chen, W., and S. Jinks-Robertson, 1999 The role of the mismatch repair machinery in regulating mitotic and meiotic recombination between diverged sequences in yeast. Genetics **151:** 1299–1313.

Chiurazzi, M., A. Ray, J. F. Viret, R. Perera, X. H. Wang *et al.*, 1996 Enhancement of somatic intrachromosomal homologous

recombination in Arabidopsis by the HO endonuclease. Plant Cell **8:** 2057–2066.

Chomet, P., D. Lisch, K. J. Hardeman, V. L. Chandler and M. Freeling, 1991 Identification of a regulatory transposon that controls the *Mutator* transposable element system in maize. Genetics **129:** 261–270.

Chou, Q., M. Russell, D. E. Birch, J. Raymond and W. Bloch, 1992 Prevention of pre-PCR mis-priming and primer dimerization improves low-copy-number amplifications. Nucleic Acids Res. **20:** 1717–1723.

Civardi, L., Y. Xia, K. J. Edwards, P. S. Schnable and B. J. Nikolau, 1994 The relationship between genetic and physical distances in the cloned *a1-sh2* interval of the *Zea mays* L. genome. Proc. Natl. Acad. Sci. USA **91:** 8268–8272.

Collins, I., and C. S. Newlon, 1994 Meiosis-specific formation of joint DNA molecules containing sequences from homologous chromosomes. Cell **76:** 65–75.

de Massy, B., and A. Nicolas, 1993 The control in *cis* of the position and the amount of the *ARG4* meiotic double-strand break of *Saccharomyces cerevisiae*. EMBO J. **12:** 1459–1466.

Detloff, P., M. A. White and T. D. Petes, 1992 Analysis of a gene conversion gradient at the *HIS4* locus in *Saccharomyces cerevisiae*. Genetics **132:** 113–123.

Dooner, H. K., 1986 Genetic fine structure of the *bronze* locus in maize. Genetics **113:** 1021–1036.

Dooner, H. K., 2002 Extensive interallelic polymorphisms drive meiotic recombination into a crossover pathway. Plant Cell **14:** 1173–1183.

Dooner, H. K., and I. M. Martinez-Ferez, 1997a Germinal excisions of the maize transposon *activator* do not stimulate meiotic recombination or homology-dependent repair at the *bz* locus. Genetics **147:** 1923–1932.

Dooner, H. K., and I. M. Martinez-Ferez, 1997b Recombination occurs uniformly within the *bronze* gene, a meiotic recombination hotspot in the maize genome. Plant Cell **9:** 1633–1646.

Eggleston, W. B., M. Alleman and J. L. Kermicle, 1995 Molecular organization and germinal instability of *R-stippled* maize. Genetics **141:** 347–360.

Elliott, B., C. Richardson, J. Winderbaum, J. A. Nickoloff and M. Jasin, 1998 Gene conversion tracts from double-strand break repair in mammalian cells. Mol. Cell. Biol. **18:** 93–101.

Fan, Q., F. Xu and T. D. Petes, 1995 Meiosis-specific double-strand DNA breaks at the *HIS4* recombination hot spot in the yeast *Saccharomyces cerevisiae*: control in *cis* and *trans*. Mol. Cell. Biol. **15:** 1679–1688.

Game, J. C., 1992 Pulsed-field gel analysis of the pattern of DNA double-strand breaks in the Saccharomyces genome during meiosis. Dev. Genet. **13:** 485–497.

Gerton, J. L., J. DeRisi, R. Shroff, M. Lichten, P. O. Brown *et al.*, 2000 Inaugural article: global mapping of meiotic recombination hotspots and coldspots in the yeast Saccharomyces cerevisiae. Proc. Natl. Acad. Sci. USA **97:** 11383–11390.

Gloor, G. B., N. A. Nassif, D. M. Johnson-Schlitz, C. R. Preston and W. R. Engels, 1991 Targeted gene replacement in Drosophila via P element-induced gap repair. Science **253:** 1110–1117.

Goyon, C., and M. Lichten, 1993 Timing of molecular events in meiosis in Saccharomyces cerevisiae: stable heteroduplex DNA is formed late in meiotic prophase. Mol. Cell. Biol. **13:** 373–382.

Hershberger, R. J., C. A. Warren and V. Walbot, 1991 Mutator activity in maize correlates with the presence and expression of the Mu transposable element Mu9. Proc. Natl. Acad. Sci. USA **88:** 10198–10202.

Hilliker, A. J., G. Harauz, A. G. Reaume, M. Gray, S. H. Clark *et al.*, 1994 Meiotic gene conversion tract length distribution within the rosy locus of *Drosophila melanogaster*. Genetics **137:** 1019–1026.

Holliday, R., 1964 A mechanism for gene conversion in fungi. Genet. Res. **78:** 282–304.

Hsia, A. P., and P. S. Schnable, 1996 DNA sequence analyses support the role of interrupted gap repair in the origin of internal deletions of the maize transposon, MuDR. Genetics **142:** 603–618.

Hunter, N., and N. Kleckner, 2001 The single-end invasion: an asymmetric intermediate at the double-strand break to double-Holliday junction transition of meiotic recombination. Cell **106:** 59–70.

Jiang, N., C. Feschotte, X. Zhang and S. R. Wessler, 2004 Using rice to understand the origin and amplification of miniature inverted repeat transposable elements (MITEs). Curr. Opin. Plant Biol. **7:** 115–119.

Kim, S. H., and V. Walbot, 2003 Deletion derivatives of the MuDR regulatory transposon of maize encode antisense transcripts but are not dominant-negative regulators of mutator activities. Plant Cell **15:** 2430–2447.

Kuzminov, A., 2001 Single-strand interruptions in replicating chromosomes cause double-strand breaks. Proc. Natl. Acad. Sci. USA **98:** 8241–8246.

Lee, G. S., M. B. Neiditch, S. S. Salus and D. B. Roth, 2004 RAG proteins shepherd double-strand breaks to a specific pathway, suppressing error-prone repair, but RAG nicking initiates homologous recombination. Cell **117:** 171–184.

Lee, M., N. Sharopova, W. D. Beavis, D. Grant, M. Katt *et al.*, 2002 Expanding the genetic map of maize with the intermated B73 × Mo17 (IBM) population. Plant Mol. Biol. **48:** 453–461.

Levy, A. A., and V. Walbot, 1991 Molecular analysis of the loss of somatic instability in the bz2::mu1 allele of maize. Mol. Gen. Genet. **229:** 147–151.

Levy, A. A., A. B. Britt, K. R. Luehrsen, V. L. Chandler, C. Warren *et al.*, 1989 Developmental and genetic aspects of Mutator excision in maize. Dev. Genet. **10:** 520–531.

Li, Y., J. P. Bernot, C. Illingworth, W. Lison, K. M. Bernot *et al.*, 2001 Gene conversion within regulatory sequences generates maize r alleles with altered gene expression. Genetics **159:** 1727–1740.

Lichten, M., and A. S. Goldman, 1995 Meiotic recombination hotspots. Annu. Rev. Genet. **29:** 423–444.

Lichten, M., C. Goyon, N. P. Schultes, D. Treco, J. W. Szostak *et al.*, 1990 Detection of heteroduplex DNA molecules among the products of Saccharomyces cerevisiae meiosis. Proc. Natl. Acad. Sci. USA **87:** 7653–7657.

Lisch, D., 2002 Mutator transposons. Trends Plant Sci. **7:** 498–504.

Lisch, D., P. Chomet and M. Freeling, 1995 Genetic characterization of the *Mutator* system in maize: behavior and regulation of *Mu* transposons in a minimal line. Genetics **139:** 1777–1796.

Liu, J., T. C. Wu and M. Lichten, 1995 The location and structure of double-strand DNA breaks induced during yeast meiosis: evidence for a covalently linked DNA-protein intermediate. EMBO J. **14:** 4599–4608.

Lowe, B., J. Mathern and S. Hake, 1992 Active Mutator elements suppress the knotted phenotype and increase recombination at the Kn1-O tandem duplication. Genetics **132:** 813–822.

Mathern, J., and S. Hake, 1997 Mu element-generated gene conversions in maize attenuate the dominant knotted phenotype. Genetics **147:** 305–314.

Nag, D. K., and T. D. Petes, 1993 Physical detection of heteroduplexes during meiotic recombination in the yeast Saccharomyces cerevisiae. Mol. Cell. Biol. **13:** 2324–2331.

Newton, C. R., A. Graham, L. E. Heptinstall, S. J. Powell, C. Summers *et al.*, 1989 Analysis of any point mutation in DNA. The amplification refractory mutation system (ARMS). Nucleic Acids Res. **17:** 2503–2516.

Nickoloff, J. A., D. B. Sweetser, J. A. Clikeman, G. J. Khalsa and S. L. Wheeler, 1999 Multiple heterologies increase mitotic double-strand break-induced allelic gene conversion tract lengths in yeast. Genetics **153:** 665–679.

O'Reilly, C., N. S. Shepherd, A. Pereira, Z. Schwarz-Sommer, I. Bertram *et al.*, 1985 Molecular cloning of the *a1* locus of *Zea mays* using the transposable elements *En* and *Mu1*. EMBO J. **4:** 877–882.

Palmer, S., E. Schildkraut, R. Lazarin, J. Nguyen and J. A. Nickoloff, 2003 Gene conversion tracts in Saccharomyces cerevisiae can be extremely short and highly directional. Nucleic Acids Res. **31:** 1164–1173.

Patterson, G. I., K. M. Kubo, T. Shroyer and V. L. Chandler, 1995 Sequences required for paramutation of the maize b gene map to a region containing the promoter and upstream sequences. Genetics **140:** 1389–1406.

Preston, C. R., and W. R. Engels, 1996 *P*-element-induced male recombination and gene conversion in Drosophila. Genetics **144:** 1611–1622.

Puchta, H., and B. Hohn, 1996 From centiMorgans to base pairs: homologous recombination in plants. Trends Genet. **1:** 340–348.

Puchta, H., B. Dujon and B. Hohn, 1993 Homologous recombination in plant cells is enhanced by in vivo induction of double strand breaks into DNA by a site-specific endonuclease. Nucleic Acids Res. **21:** 5034–5040.

Puchta, H., B. Dujon and B. Hohn, 1996 Two different but related mechanisms are used in plants for the repair of genomic double-strand breaks by homologous recombination. Proc. Natl. Acad. Sci. USA **93:** 5055–5060.

Qin, M. M., D. S. Robertson and A. H. Ellingboe, 1991 Cloning of the Mutator transposable element MuA2, a putative regulator of somatic mutability of the a1-Mum2 allele in maize. Genetics **129:** 845–854.

Raizada, M. N., M. I. Benito and V. Walbot, 2001a The MuDR transposon terminal inverted repeat contains a complex plant promoter directing distinct somatic and germinal programs. Plant J. **25:** 79–91.

Raizada, M. N., G. L. Nan and V. Walbot, 2001b Somatic and germinal mobility of the RescueMu transposon in transgenic maize. Plant Cell **13:** 1587–1608.

Resnick, M. A., 1976 The repair of double-strand breaks in DNA; a model involving recombination. J. Theor. Biol. **59:** 97–106.

Robertson, D. S., and P. S. Stinard, 1993 Evidence for *Mu* activity in the male and female gametophytes of maize. Maydica **38:** 145–150.

Schnable, P. S., and P. A. Peterson, 1986 Distribution of genetically active *Cy* elements among diverse maize lines. Maydica **31:** 59–82.

Schnable, P. S., P. A. Peterson and H. Saedler, 1989 The *bz-rcy* allele of the *Cy* transposable element system of *Zea mays* contains a *Mu*-like element insertion. Mol. Gen. Genet. **217:** 459–463.

Schnable, P. S., A. P. Hsia and B. J. Nikolau, 1998 Genetic recombination in plants. Curr. Opin. Plant Biol. **1:** 123–129.

Schultes, N. P., and J. W. Szostak, 1990 Decreasing gradients of gene conversion on both sides of the initiation site for meiotic recombination at the ARG4 locus in yeast. Genetics **126:** 813–822.

Schwacha, A., and N. Kleckner, 1994 Identification of joint molecules that form frequently between homologs but rarely between sister chromatids during yeast meiosis. Cell **76:** 51–63.

Schwacha, A., and N. Kleckner, 1995 Identification of double Holliday junctions as intermediates in meiotic recombination. Cell **83:** 783–791.

Schwarzacher, T., 2003 Meiosis, recombination and chromosomes: a review of gene isolation and fluorescent in situ hybridization data in plants. J. Exp. Bot. **54:** 11–23.

Smith, G. R., 2001 Homologous recombination near and far from DNA breaks: alternative roles and contrasting views. Annu. Rev. Genet. **35:** 243–274.

Stinard, P. S., D. S. Robertson and P. S. Schnable, 1993 Genetic isolation, cloning, and analysis of a mutator-induced, dominant antimorph of the maize amylose extender1 locus. Plant Cell **5:** 1555–1566.

Sun, H., D. Treco, N. P. Schultes and J. W. Szostak, 1989 Double-strand breaks at an initiation site for meiotic gene conversion. Nature **338:** 87–90.

Sun, H., D. Treco and J. W. Szostak, 1991 Extensive 3′-overhanging, single-stranded DNA associated with the meiosis-specific double-strand breaks at the ARG4 recombination initiation site. Cell **64:** 1155–1161.

Sweetser, D. B., H. Hough, J. F. Whelden, M. Arbuckle and J. A. Nickoloff, 1994 Fine-resolution mapping of spontaneous and double-strand break-induced gene conversion tracts in Saccharomyces cerevisiae reveals reversible mitotic conversion polarity. Mol. Cell. Biol. **14:** 3863–3875.

Szostak, J. W., T. L. Orr-Weaver, R. J. Rothstein and F. W. Stahl, 1983 The double-strand-break repair model for recombination. Cell **33:** 25–35.

Walbot, V., and G. N. Rudenko, 2002 MuDR/Mu transposable elements of maize, pp. 533–564 in *Mobile DNA II*, edited by N. L. Craig, R. Craigie, M. Gellert and A. M. Lambowitz. ASM Press, Washington, DC.

Weil, C. F., and R. Kunze, 2000 Transposition of maize Ac/Ds transposable elements in the yeast Saccharomyces cerevisiae. Nat. Genet. **26:** 187–190.

White, J. H., K. Lusnak and S. Fogel, 1985 Mismatch-specific postmeiotic segregation frequency in yeast suggests a heteroduplex recombination intermediate. Nature **315:** 350–352.

Xiao, Y. L., and T. Peterson, 2000 Intrachromosomal homologous recombination in Arabidopsis induced by a maize transposon. Mol. Gen. Genet. **263:** 22–29.

Xiao, Y. L., X. Li and T. Peterson, 2000 Ac insertion site affects the frequency of transposon-induced homologous recombination at the maize p1 locus. Genetics **156:** 2007–2017.

Xu, X., A. P. Hsia, L. Zhang, B. J. Nikolau and P. S. Schnable, 1995 Meiotic recombination break points resolve at high rates at the 5′ end of a maize coding sequence. Plant Cell **7:** 2151–2161.

Yao, H., Q. Zhou, J. Li, H. Smith, M. Yandeau *et al.*, 2002 Molecular characterization of meiotic recombination across the 140-kb multigenic a1-sh2 interval of maize. Proc. Natl. Acad. Sci. USA **99:** 6157–6162.

Yeadon, P. J., and D. E. Catcheside, 1998 Long, interrupted conversion tracts initiated by cog in Neurospora crassa. Genetics **148:** 113–122.

Yu, J., K. Marshall, M. Yamaguchi, J. E. Haber and C. F. Weil, 2004 Microhomology-dependent end joining and repair of transposon-induced DNA hairpins by host factors in Saccharomyces cerevisiae. Mol. Cell. Biol. **24:** 1351–1364.

Zenvirth, D., T. Arbel, A. Sherman, M. Goldway, S. Klein *et al.*, 1992 Multiple sites for double-strand breaks in whole meiotic chromosomes of Saccharomyces cerevisiae. EMBO J. **11:** 3441–3447.

Communicating editor: J. A. Birchler

APPENDIX

Positions of the recombination breakpoints associated with the *A1′* alleles isolated from crosses 1 and 2

Allele[a]	Cross	Position of breakpoint/5′ endpoint[b]	Position of 3′ endpoint	Type of recombination
94B 129	2	ND[c]	NA	Crossover
94B 131	2	VII	XXIII	Gene conversion
94B 132	2	XXI	XXIII	Gene conversion
94B 133	2	V	NA	Crossover
94B 135	2	ND	NA	Crossover
94B 136	2	VII	NA	Crossover
94B 139	2	XIII	NA	Crossover
94B 140	2	I	NA	Crossover
94B 141	2	I	NA	Crossover
94B 142	2	V	NA	Crossover
94B 143	2	VII	NA	Crossover
94B 145	2	ND	NA	Crossover
94B 146	2	VII	NA	Crossover
94B 149	2	VII	NA	Crossover
94B 150	2	V	NA	Crossover
94B 151	2	V	NA	Crossover
94B 152	2	VII	NA	Crossover
94B 153	2	VII	NA	Crossover
94B 154	2	VII	NA	Crossover
94B 156	2	I	3′ of XXIII	Gene conversion
94B 158	2	VII	NA	Crossover
94B 161	2	V	NA	Crossover
94B 164	2	VII	NA	Crossover
94B 166	2	XIII	NA	Crossover
94B 168	2	XXI	3′ of XXIII	Gene conversion
94B 169	2	VII	NA	Crossover
94B 170	2	VII	NA	Crossover
94B 173	2	V	NA	Crossover
94B 176	2	V	NA	Crossover
94B 177	2	VII	XXIII	Gene conversion
94B 179	2	VII	NA	Crossover
94B 185	2	XIII	NA	Crossover
94B 188	1	II	NA	Crossover
94B 190	1	VII	NA	Crossover
94B 192	1	VII	NA	Crossover
94B 195	1	VII	3′ of XXIII	Gene conversion
94B 198	1	V	3′ of XXIII	Gene conversion
94B 199	1	XV	NA	Crossover
94B 200	1	VII	XXIII	Gene conversion
94B 202	1	ND	NA	Crossover

NA, not applicable.

[a] All of the *A1′* alleles from Table 1 that were confirmed by RFLP analysis are listed.

[b] Intervals as shown in Figure 2.

[c] Not determined because the associated *A1′* allele failed to PCR amplify.